Symmetry of the spin Hamiltonian for herbertsmithite: A spin-$\frac{1}{2}$ kagome lattice

Oren Ofer and Amit Keren

Department of Physics, Technion, Israel Institute of Technology, Haifa 32000, Israel

(Received 29 July 2008; revised manuscript received 7 October 2008; published 20 April 2009)

We present magnetization measurements on oriented powder of $ZnCu_3(OH)_6Cl_2$ along and perpendicular to the orienting field. We find a dramatic difference in the magnetization between the two directions. It is biggest at low measurement fields H or high temperatures. We show that the difference at high temperatures must emerge from the Ising-type exchange anisotropy. This allows us to explain muon spin rotation data at $T \to 0$ in terms of an exotic ferromagnetic ground state.

The synthesis of herbertsmithite $[ZnCu_3(OH)_6Cl_2]$ (Ref. 1) has led to a renewed interest in the frustrated spin-1/2 Heisenberg model on the kagome lattice. This system has a highly degenerate ground state[2] and any small perturbation to the Hamiltonian can severely affect the ground-state manifold. The perturbations can be exchange anisotropy,[3] bond anisotropy,[4,5] transverse field (TF),[6,7] Dzyaloshinksy-Moriya interaction (DMI),[8–10] or longer-range interactions.[11] Therefore, numerous theoretical directions have been taken to predict the low-temperature behavior of the kagome system, and some of them were particularly applied to magnetization and other measurements of herbertsmithite.[10,12]

This mithite is exciting since Cu ions create a spin-1/2 magnetic kagomé layer separated by nonmagnetic Zn atoms from the adjacent layers. The compound was found to be a quantum spin liquid with no broken continuous symmetry but gapless excitations.[13–17] At high temperatures, the inverse susceptibility obeys a Curie-Weiss (CW) law $\chi = C/(T+\theta)$, where C is the Curie constant and the CW temperature $\theta = 314$ K. Below ~ 75 K, a sharp increase in the susceptibility occurs, deviating from the ideal kagome Heisenberg model.[18] This upturn was accounted for by DMI (Refs. 10 and 19) or anisotropy in the bonds.[4,7] It was also suggested that impurities from a Zn/Cu substitution play a significant role in the low-temperature susceptibility.[17,20,21] However, free impurities or interacting impurities that generate an additional ferromagnetic Curie-Weiss law[10,12] have been shown not to describe this upturn completely. In fact, Rietveld refinement of our sample showed no Zn/Cu substitution within the experimental resolution.[22] The sample is made by the same procedure and group as the samples in Refs. 15 and 23. Finally, different local probes such as muon,[14] O,[17] Cu, and Cl (Ref. 23) nuclear-magnetic resonance, and electron-spin resonance[19] suggest different behavior of the susceptibility below ~ 50 K. Thus, there is still no agreement on the interactions that control the magnetic properties of herbertsmithite.

In fact, since it is only available as a powder, the symmetries of its spin Hamiltonian are not known. To clarify these symmetries, we present magnetization measurements on oriented powder of $ZnCu_3(OH)_6Cl_2$ along ($\hat{z}$) and perpendicular to ($\perp$) the orienting field. The symmetry of the interactions is probed at high temperatures where impurities are not expected to contribute to the susceptibility even if they do exist, and all probes roughly agree.

The orientation was done by curing $ZnCu_3(OH)_6Cl_2$ powder overnight with Stycast in a field of 8 T at room temperature. The samples were cured in a Teflon form producing a ball 6 mm in diameter. During the first 40 min of the orientation, a shaking mechanism was applied to the sample form. A particularly small amount of powder was used to avoid saturating the Stycast and eliminating powder residues at the bottom of the ball. We prepared a second "test" sample in the same manner, but this time without orientation. We refer to the second ball as the powder sample. The mass of $ZnCu_3(OH)_6Cl_2$ in the ball is known only roughly and the absolute value of the molar magnetization is not accurate. We also prepared a ball made of Stycast only. All samples were measured in a gelatin capsule.

In Fig. 1 we plot the x-ray diffraction from the powder and oriented samples. For these measurements, a separate surface perpendicular to the orienting field was prepared and used. The Bragg-peak intensities are shown in the figure. In the oriented case, the (002) and (006) peaks increased dramatically, while many of the other peaks did not. This x-ray picture shows a high degree of orientation such that the c direction is parallel to the field. The level of orientation will be discussed further below.

dc magnetization measurements M were performed using a cryogenic superconducting quantum interference device
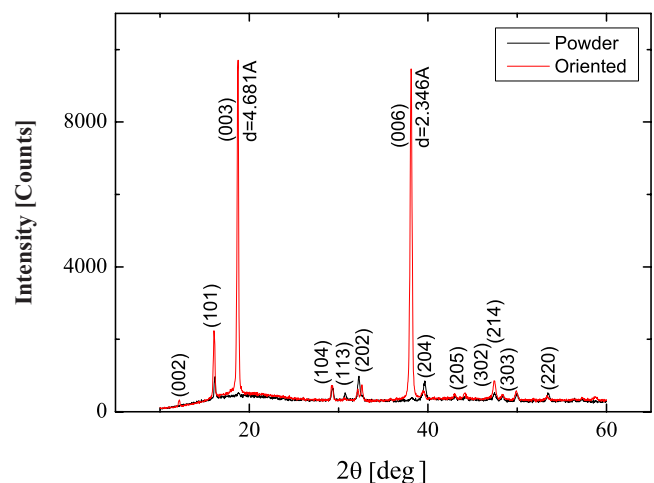

FIG. 1. (Color online) X-ray diffraction of powder (black) and oriented powder (gray) from a surface perpendicular to the orienting field.
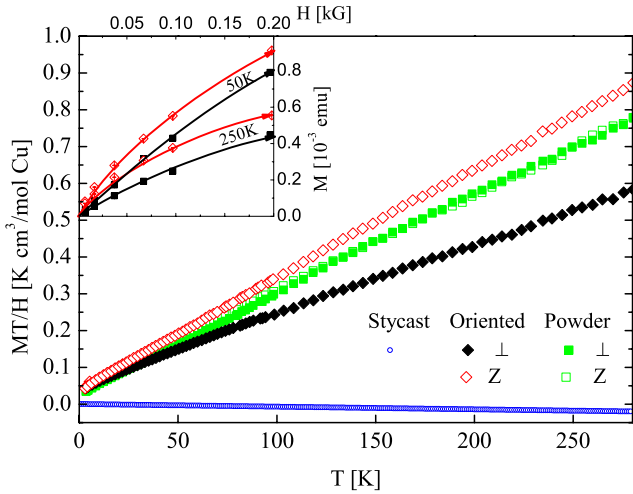
FIG. 2. (Color online) Normalized magnetization $M/H \equiv \chi$ times the temperature versus temperature at external field of 400 G for oriented sample (diamonds) in two directions, powder sample (squares) in two directions as if it was oriented, and Stycast sample (open circles). The inset shows the magnetization as a function of the applied field for two different temperatures and directions for low fields.

(SQUID) magnetometer in two configurations. One configuration "z" is when the orienting and the applied (SQUID) fields coincide ($H \| c$). The other configuration "$\perp$" is when the ball is rotated by 90° and thus the applied field is in the kagomé plane ($H \perp c$). In Fig. 2 we present MT/H of the two samples: powder and oriented balls. In the reset of this paper, we use χ to indicate the normalized magnetization M/H (and not $\partial M/\partial H$). These measurements were taken at $H = 400$ G. The measurements are conducted as follows. We first measured the powder sample and then the oriented sample in both configurations. Finally, we repeated the powder measurements for a second time but rotated the powder ball as if it was oriented. All powder measurements collapse into a single curve, as expected, demonstrating the reproducibility of the measurement. The Stycast sample showed a very small diamagnetic signal which is also depicted in Fig. 2. The core diamagnetic susceptibility of $ZnCu_3(OH)_6Cl_2$ is -16.7×10^{-5} cm^3/mol.[24] The Van Vleck contribution is expected to be of the same order of magnitude but with a positive sign.[25] Both are much smaller than the measured χ at room temperature of 1×10^{-3} cm^3/mol.

In Fig. 2, no special energy scale is found in either one of the measurements. The only indication of an interaction between spins is the fact that χT for both directions and the powder decreases with decreasing T. χT of the powder is smaller than $\chi_z T$ and larger than $\chi_\perp T$ of the oriented sample. However, a comparison of the absolute value of χ of the powder and the oriented sample is not accurate. We did try to have an equal amount of sample in both balls but there is no telling how successful we were. A more relevant comparison is between χ in the different directions of the oriented sample; $\chi_z T$ increases faster than $\chi_\perp T$, and at room temperature $\chi_z = 1.6\chi_\perp$. Thus the ratio between the z and $\perp$ directions increases as the temperature increases.

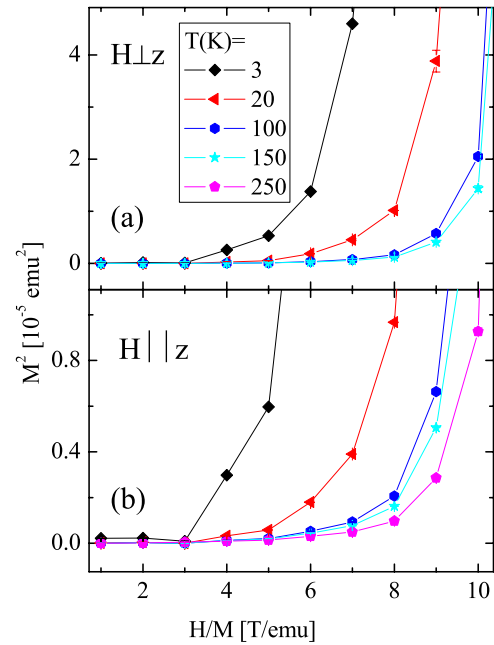In the inset of Fig. 2, we show the magnetization as a

FIG. 3. (Color online) An Arrott plot showing M^2 versus H/M at various temperatures in the perpendicular direction (a) and parallel direction (b).

function of H for two different temperatures and directions. The magnetization is beginning to show signs of saturation, suggesting contribution from ferromagnetic impurities. To check this possibility, we present in Fig. 3 an Arrott plot.[26] This plot takes advantage of the high-field data. At a ferromagnetic transition, $M^2(T_c)$ is expected to be a linear function of H/M. We found no evidence for such linear behavior. In fact, $M^2(T)$ is independent of H/M near the origin as expected when the ferromagnetic critical temperature is lower than the available temperature. This indicates the lack of ferromagnetic impurities in our measurements.

In Fig. 4 we plot χ^{-1} versus temperature for two fields 2000 and 100 G and for the two orientations. In the inset of Fig. 4(b) we plot the χ^{-1} at low temperatures ($T < 50$ K); clearly, χ_z linearizes at $T \sim 30$ K whereas $\chi^\perp$ linearizes at a much higher temperature ($T \sim 100$ K). θ and C in arbitrary units are extracted from a linear fit of the high-temperature ($150 < T < 280$ K) data to $\chi_{\perp,z}^{-1} = (T + \theta_{\perp,z})/C_{\perp,z}$. The fits are shown by the solid line.

In Fig. 5 we plot $\theta_{\perp,z}$ and $\sqrt{C_{\perp,z}}$ which is proportional to the $g_{\perp,z}$ factor (if the sample was fully oriented) versus the applied field. $\theta_\perp$ increases slowly with decreasing applied field and saturates below 400 G. On the other hand, θ_z increases rapidly below 2 kG. The Curie constant has a similar behavior. The powder average of $\theta_{\perp,z}$ at low fields does not reconcile with $\theta \sim 300$ K measured in a powder and there must be some extrinsic contribution to the normalized magnetization in the partially aligned samples at low fields. However, we have no evidence that this contribution is due to impurities.

In contrast, at high fields $H > 2$ kG, θ of the two directions is hardly distinguishable and on the order of the powder value. In addition, useful information can be extracted from the CW temperature only if it is obtained by measurements at
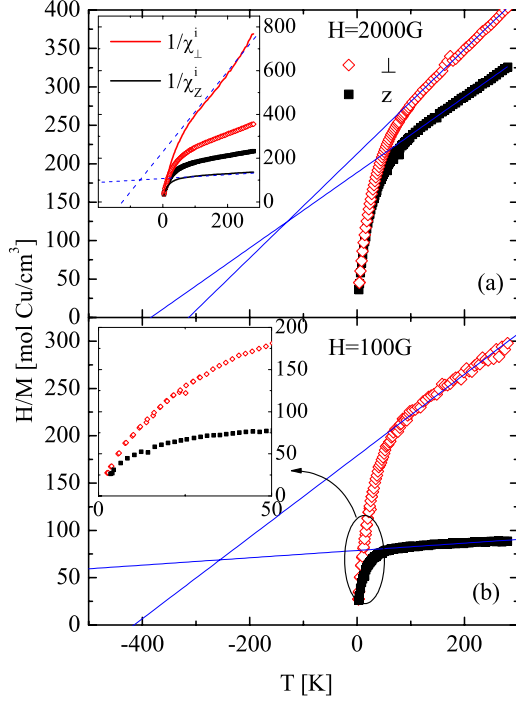
FIG. 4. (Color online) Inverse normalized magnetization $H/M \equiv \chi^{-1}$ versus temperature at (a) $H=2$ kG and at (b) $H=100$ G. The solid lines are linear fits to the high-temperature (>150 K) data. (a) Inset displays the inverse of the normalized magnetizations $1/\chi_z$ (black squares) and $1/\chi_\perp$ (gray diamonds) and the inverse intrinsic normalized magnetization $1/\chi_\perp^i$ (black line) and $1/\chi_z^i$ (gray line) obtained from Eq. (1). The dashed lines demonstrate that $\theta_z < \theta_z^i$ and $\theta_\perp > \theta_\perp^i$. In the inset of (b), we plot the low-temperature behavior of χ^{-1} at 100 G.

$T \gtrsim \theta$. Therefore, we concentrate on the results obtained by $H \geq 2$ kG, as shown in the inset of Fig. 5. At 2 kG, the ratio of $\sqrt{C_z/C_\perp} = 1.179(6)$ and $\theta_z/\theta_\perp = 1.23(1)$.

In order to convert the measured χ presented above to the intrinsic normalized magnetization χ^i in different directions, it is important to estimate the level of orientation. This can
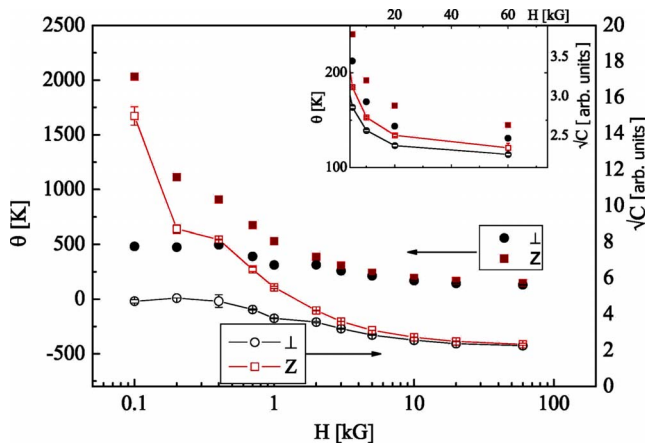

FIG. 5. (Color online) The Curie-Weiss temperatures (filled symbols) and square root of the Curie constant (open symbols) of the oriented sample perpendicular to (black) and in the kagomé plane (gray). The inset shows a zoom on the high-field data.

be done using the x-ray data. The ratio of the x-ray intensity (I) from the powder $R=I(00h)/I(kk0)$ represents the signal intensity ratio between the two kinds of plane. Let us assume that there are N grains composed of two sets: αN that can orient perfectly with the field and $(1-\alpha)N$ that are not affected by the field at all since they are made of few crystalline, for example. We further define β as the probability that a particular plane will contribute to the scattering intensity in a powder. After orientation, the x-ray intensity ratio between the same planes would be $R'=[\alpha R+\beta(1-\alpha)R]/\beta(1-\alpha)$. We can estimate β from the width of the peaks which is 0.2° out of 180, thus $\beta \sim 0.001$. Using R and R' of the (006) and (220), we find $\alpha=0.25$. This level of orientation is in agreement with Imai et al.[23]

In an oriented sample, we expect

$$\chi_{z,\perp} = (1-\alpha)\left(\frac{1}{3}\chi_z^i + \frac{2}{3}\chi_\perp^i\right) + \alpha\chi_{z,\perp}^i. \quad (1)$$

This relation could be inverted to produce $\chi_{z,\perp}^i$. In the inset of Fig. 4(a), we present both $1/\chi_{z,\perp}$ and $1/\chi_{z,\perp}^i$ for the normalized magnetization data taken at $H=2$ kG. New intrinsic CW temperatures $\theta_{z,\perp}^i$ could be obtained from $1/\chi_{z,\perp}^i$ as demonstrated by the dashed lines. $\theta_{z,\perp}^i$ represent the CW temperature as if the sample was fully oriented. Although α is just an estimate of the level of orientation, the important point is that $\theta_z^i > \theta_z$ and $\theta_\perp^i < \theta_\perp$.

We now turn to discuss the possible origin of the χ anisotropy in terms of superexchange anisotropy and DMI. The DMI Hamiltonian is given by

$$\mathcal{H} = \sum_{\langle i,j \rangle} J\mathbf{S}_i \cdot \mathbf{S}_j + \mathbf{D}_{ij} \cdot (\mathbf{S}_i \times \mathbf{S}_j), \quad (2)$$

where $\mathbf{D}_{ij}$ is a vector assigned to each bond. In the mean-field approximation $(\mathbf{S}_j \rightarrow \mathbf{M}/g\mu_B)$ this Hamiltonian is written as

$$\mathcal{H} = g\mu_B \sum_i \mathbf{S}_i \cdot \mathbf{H}^{\text{eff}},$$

where

$$\mathbf{H}^{\text{eff}} = \frac{Z}{(g\mu_B)^2}(J\mathbf{M} + \mathbf{D} \times \mathbf{M}) + \mathbf{H}, \quad (3)$$

$\mathbf{D}=(1/Z)\Sigma_j\mathbf{D}_{ij}$, and Z is the number of neighbors. Special attention must be taken for the convention of the ij bond direction since it sets the direction of $\mathbf{D}_{ij}$.[10] The magnetization satisfies the equation

$$\mathbf{M} = \frac{C}{T}\left[\frac{Z}{(g\mu_B)^2}(J\mathbf{M} + \mathbf{D} \times \mathbf{M}) + \mathbf{H}\right], \quad (4)$$

where $C=(g\mu_B)^2 S(S+1)/(3k_B)$ is the Curie constant. Up to the first order in $\mathbf{D}$,

$$\mathbf{M} = \frac{C}{(T - \theta_{cw})}\left(I + \frac{1}{T - \theta_{cw}}\mathbf{A}\right)\mathbf{H}, \quad (5)$$

where $\theta_{\text{CW}}=CZJ/(g\mu_B)^2$ and

$$\mathbf{A} = \frac{CZ}{(g\mu_B)^2} \begin{pmatrix} 0 & -D_z & D_y \\ D_z & 0 & -D_x \\ -D_y & D_x & 0 \end{pmatrix}. \tag{6}$$

In particular,

$$M_{z,\perp} = \frac{C}{(T - \theta_{CW})} H_{z,\perp}. \tag{7}$$

Therefore, $\mathbf{D}_{ij}$ does not contribute to the CW law.

In contrast, the superexchange anisotropy Hamiltonian is given by

$$\mathcal{H} = \sum_{\langle i,j \rangle} J_z S_i^z \cdot S_j^z + J_\perp \mathbf{S}_i^\perp \cdot \mathbf{S}_j^\perp. \tag{8}$$

In this case, if the sample was perfectly oriented, we would have $\theta_{z,\perp} = J_{z,\perp}/k_B$. Since our sample is not perfectly oriented, our high-temperature high-field linear fits of $\chi_{\perp,z}^{-1}$ measure a lower bound on J_z and an upper bound on $J_\perp$.

The lower bound on J_z is larger than the upper bound on $J_\perp$. Despite the fact that measurements of χ_z and $\chi_\perp$ are contaminated with $\chi_\perp^i$ and χ_z^i, respectively, as indicated by Eq. (1), the conclusion $J_z > J_\perp$ is unavoidable. It is robust even against possible core and Van Vleck corrections. Thus herbertsmithite has an Ising-type exchange anisotropy. This, however, is not the end of the story. If $J_z > J_\perp$, we would expect $\chi_z < \chi_\perp$, in contrast to the observation. Therefore, to explain the high χ in the z direction, we must invoke an anisotropic g factor as well.

In the classical ground state of antiferromagnets on the kagomé lattice with exchange anisotropy, the spins are coplanar and two angles between spins φ on each triangle obey $\cos \varphi = -J_z/(J_z + J_\perp)$. The third angle completes the circle. This condition maintains the ground-state macroscopic degeneracy. Nevertheless, unlike in the Heisenberg case, there is a critical temperature T_c below which an exotic ferromagnetic order exists with finite total magnetization but no sublattice long-range order.[27] Upon cooling through T_c, the magnetization increases abruptly and continuously down to $T \rightarrow 0$ where it saturates.[28] In zero field, domains can be formed, but a small applied magnetic field will stabilize the moment. The powder average of the moment projection on the field direction is given by the value

$$\langle \mathbf{M} \cdot \hat{\mathbf{H}} \rangle = \frac{\mu_B}{6}(1 + 2 \cos \varphi) \tag{9}$$

per spin.

We believe that this ferromagnetic order contributes to the observed χ at $T \rightarrow 0$ by TF muon spin rotation (μSR) experiment.[14] In μSR, impurities—if they exist—are expected to contribute to the muon line width while most of the sample contributes to the line shift. In what follows, we examine what part of the μSR shift can be explained by exchange anisotropy only. A complete understanding will of course require taking DMI interaction into account as well.

The μSR measurements were done at a field of $H = 2$ kG and the shift K in the muon rotation frequency as a function of temperature was measured. This shift is a conse-
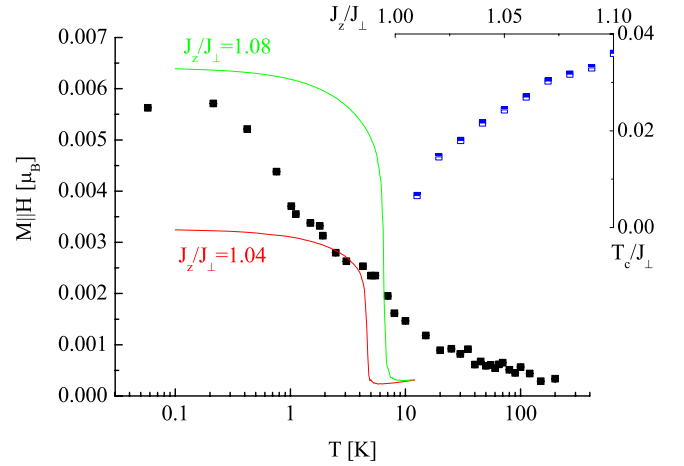

FIG. 6. (Color online) A plot of the magnetization detected by the muon spin rotation versus temperature (black squares) and simulation data for antiferromagnetic kagomé lattice with Ising-type exchange anisotropy as in Ref. 28 (gray lines). In the inset, the normalized critical temperature versus exchange anisotropy is shown.

quence of the sample magnetization; therefore, K is expected to be proportional to the normalized magnetization. The high-temperature data are used to calibrate the proportionality constant between K and χ.[14] The data are reproduced in Fig. 6. χ increases sharply with decreasing temperatures between ~ 10 K and ~ 1 K and saturates below $T \sim 200$ mK at a value of $\chi = 15.7(5) \times 10^{-3}$ cm^3/mol Cu. This χ amounts to an average moment of $0.006\mu_B$ per Cu, in the direction of the applied 2 kG field. Solving Eq. (9) for the anisotropies gives $J_z/J_\perp = 1.06$. In Fig. 6 we present simulations described in Ref. 27 for $J_z/J_\perp = 1.04$ and $J_z/J_\perp = 1.08$, showing similar behavior as the experiment. For this type of exchange anisotropy, the expected $T_c/J_\perp = 0.03$, as shown in the inset of Fig. 6, also taken from Ref. 27. For $J_\perp \simeq 200$ K, we expect $T_c = 6$ K. This temperature is at the center of the sharp rise of χ. Thus we see that both the saturation and the increase of χ detected by μSR could be qualitatively explained by exchange anisotropy.

To summarize, our measurements in ZnCu$_3$(OH)$_6$Cl$_2$ reveal an anisotropic intrinsic spin magnetization with $\chi_z^i > \chi_\perp^i$ possibly due to an anisotropic g factor. At fields above 2 kG, a CW temperature can be consistently determined in two different directions. By mean-field approximations, we were able to show that this phenomenon can be explained only by anisotropic superexchange constants where $J_z > J_\perp$. This anisotropy can explain the main features of the susceptibility determined by μSR.

[1] M. P. Shores, E. A. Nytko, B. M. Bartlett, and D. G. Nocera, J. Am. Chem. Soc. **127**, 13462 (2005).

[2] A. P. Ramirez, Annu. Rev. Mater. Sci. **24**, 453 (1994).

[3] O. A. Starykh and L. Balents, Phys. Rev. Lett. **93**, 127202 (2004).

[4] Philippe Sindzingre, arXiv:0707.4264 (unpublished).

[5] T. Yavors'kii, W. Apel, and H.-U. Everts, Phys. Rev. B **76**, 064430 (2007).

[6] R. Moessner, S. L. Sondhi, and P. Chandra, Phys. Rev. Lett. **84**, 4457 (2000).

[7] C.-H. Chern and M. Tsukamoto, Phys. Rev. B **77**, 172404 (2008).

[8] M. Elhajal, B. Canals, and C. Lacroix, Phys. Rev. B **66**, 014422 (2002).

[9] D. Grohol, K. Matan, J.-H. Cho, S.-H. Lee, J. W. Lynn, D. G. Nocera, and Y. S. Lee, Nature Mater. **4**, 323 (2005).

[10] Marcos Rigol and Rajiv R. P. Singh, Phys. Rev. B **76**, 184403 (2007).

[11] M. D. Núñez-Regueiro, C. Lacroix, and B. Canals, Phys. Rev. B **54**, R736 (1996).

[12] Grégoire Misguich and Philippe Sindzingre, Eur. Phys. J. B **59**, 305 (2007).

[13] S.-H. Lee, H. Kikuchi, Y. Qiu, B. Lake, Q. Huang, K. Habicht, and K. Kiefer, Nature Mater. **6**, 853 (2007).

[14] O. Ofer, A. Keren, E. A. Nytko, M. P. Shores, B. M. Bartlett, D. G. Nocera, C. Baines, and A. Amato, arXiv:cond-mat/0610540 (unpublished).

[15] J. S. Helton, K. Matan, M. P. Shores, E. A. Nytko, B. M. Bartlett, Y. Yoshida, Y. Takano, A. Suslov, Y. Qiu, J.-H. Chung, D. G. Nocera, and Y. S. Lee, Phys. Rev. Lett. **98**, 107204 (2007).

[16] P. Mendels, F. Bert, M. A. de Vries, A. Olariu, A. Harrison, F. Duc, J. C. Trombe, J. S. Lord, A. Amato, and C. Baines, Phys. Rev. Lett. **98**, 077204 (2007).

[17] A. Olariu, P. Mendels, F. Bert, F. Duc, J. C. Trombe, M. A. de Vries, and A. Harrison, Phys. Rev. Lett. **100**, 087202 (2008).

[18] T. Nakamura and S. Miyashita, Phys. Rev. B **52**, 9174 (1995).

[19] A. Zorko, S. Nellutla, J. van Tol, L. C. Brunel, F. Bert, F. Duc, J. C. Trombe, M. A. de Vries, A. Harrison, and P. Mendels, Phys. Rev. Lett. **101**, 026405 (2008).

[20] F. Bert, S. Nakamae, F. Ladieu, D. L'Hote, P. Bonville, F. Duc, J.-C. Trombe, and P. Mendels, Phys. Rev. B **76**, 132411 (2007).

[21] M. A. de Vries, K. V. Kamenev, W. A. Kockelmann, J. Sanchez-Benitez, and A. Harrison, Phys. Rev. Lett. **100**, 157205 (2008).

[22] Emily A. Nytko, Ph.D. thesis, Massachusetts Institute of Technology, 2008.

[23] T. Imai, E. A. Nytko, B. M. Bartlett, M. P. Shores, and D. G. Nocera, Phys. Rev. Lett. **100**, 077203 (2008).

[24] P. W. Selwood, *Magnetochemistry*, 2nd ed. (Interscience, New York, 1956), p. 78.

[25] D. C. Johnston and J. H. Cho, Phys. Rev. B **42**, 8710 (1990).

[26] A. Arrott, Phys. Rev. **108**, 1394 (1957).

[27] A. Kuroda and S. Miyashita, J. Phys. Soc. Jpn. **64**, 4509 (1995).

[28] Shu Tanaka and Seiji Miyashita, J. Phys.: Condens. Matter **19**, 145256 (2007).